J Therm Anal Calorim (2015) 121:691–695
DOI 10.1007/s10973-015-4629-6

Study of thermal decomposition of a zinc(II) monomethyl terephthalate complex, $[Zn(CH_3O–CO–C_6H_4COO)_2(OH_2)_3]\cdot 2H_2O$

Mihaela-Diana Şerb[1] · Paul Müller[2] · Roxana Truşcă[3] · Ovidiu Oprea[1] · Florina Dumitru[1]

Received: 27 October 2014 / Accepted: 7 March 2015 / Published online: 18 March 2015

Abstract In this contribution, we report the thermal decomposition and thermo-X-ray diffraction analyses of a Zn^{II} monomethyl terephthalate complex, $[Zn(CH_3O–CO–C_6H_4COO)_2(OH_2)_3]\cdot 2H_2O$. Both XRD and temperature-dependent T-XRD patterns for the title compound in the thermal decomposition process (temperature range 30–300 °C) present diffraction peaks reminiscent of ordered, crystalline structure of the starting complex $[Zn(CH_3O–CO–C_6H_4COO)_2(OH_2)_3]\cdot 2H_2O$. Crystallization and coordination water molecules of the title complex are eliminated in successive steps, and then the anhydrous complex decomposes to ZnO (the total experimental mass loss of 84.80 % versus the theoretical mass loss, 84.23 %). The formation of ZnO of wurtzite structure (hexagonal phase, space group $P6_3mc$) as spherical nanoparticles with average size of 58 nm has been confirmed by XRD, SEM and EDX analyses performed on the final product.

Keywords Zinc complex · Monomethyl terephthalate · Thermal study · T-XRD

Electronic supplementary material The online version of this article (doi:10.1007/s10973-015-4629-6) contains supplementary material, which is available to authorized users.

✉ Florina Dumitru
d_florina@yahoo.com

[1] Faculty of Applied Chemistry and Materials Science, Politehnica University of Bucharest, Polizu 1, 011061 Bucharest, Romania

[2] Institute of Inorganic Chemistry, RWTH Aachen University, Landoltweg 1, 52074 Aachen, Germany

[3] METAV Research and Development, 31 C.A. Rosetti, Sector 2, Bucharest, Romania

Introduction

Metal carboxylates represent a class of compounds extensively studied with regard both to fundamental scientific aspects and to application-oriented problems. Potential applications of such studies include the generation of tailor-made materials with specific chemical/or physical properties e.g., porous solids for sorption, separation and catalysis, novel nonlinear optical materials, new sensor materials and coatings etc. [1–6].

Among metal carboxylates, the simplest metal formates, acetates and oxalates have been more intensely scrutinized, but other unsaturated and aromatic carboxylates have gained increased importance in the last decades.

Terephthalic acid is the simplest linear aromatic dicarboxylic acid extensively used in the synthesized metal–organic porous frameworks with various topologies [7, 8]. The synthesis of metal terephthalate complexes from metal salts and terephthalic acid dates since 1967, when thermal decomposition of the first Ni-terephthalato complex was reported [9]. Due to its chemical robustness, terephthalate, a rigid arene system, leads to compounds of high thermal stability, but the rich coordination modes (i.e., monodentate, chelating or bridging) of this versatile ligand determines a low degree of structure predictability.

In this contribution, we report the thermal decomposition and thermo-X-ray diffraction analysis of a Zn^{II} monomethyl terephthalate complex, $[Zn(CH_3O–CO–C_6H_4COO)_2(OH_2)_3]\cdot 2H_2O$, whose crystal structure has been reported by us previously [10]. For related Zn^{II} complexes with terephtalato anions as ligands, see references [8, 11–16].

Monomethyl terephthalate is a rare chemical compound, mostly used, when in salt form, as stabilizer or chain terminator in polyethylene terephthalate synthesis [17], but we chose to use it as ligand because of the end-on coordination mode that links to Zn^{II} via one carboxylate group only. This feature allows the generation of mononuclear

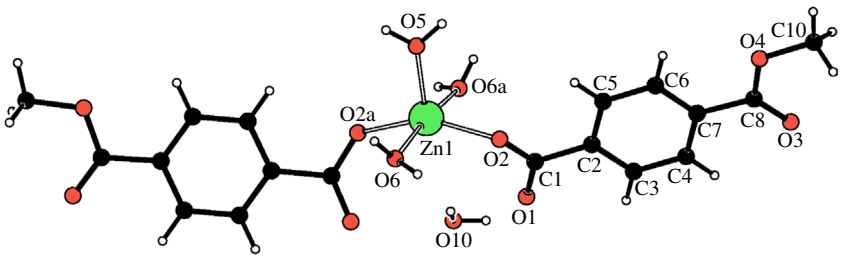

Fig. 1 Representation [19] of the title compound showing the atom-labeling scheme. Symmetry operators: $a = 1 - x, y, 1/2 - z$

complexes with ancillary labile ligands within the metal ion coordination sphere, which may serve as secondary building units in design of metal organic frameworks [18].

In our title complex, the presence of three labile water molecules as ligands for Zn^{II} suggests that they might be replaced by other ligands with different hydrogen bonding characteristics and therefore there are created premises to further increase the dimensionality of the structure.

The complex crystallizes in the space group *C2/c*, with half a molecule in the asymmetric unit, and the coordination sphere of Zn is distorted square-pyramidal: Zn(II) cation is coordinated by five O atoms, two from the monodentate methylterephthalato group and three from water molecules (Fig. 1); one water molecule is situated in apical position. A number of classical intermolecular O–H···O hydrogen bonds stabilize the crystal structure of this compound [10].

Starting from these considerations, we carried out TG-DSC and thermo-X-ray diffraction experiments to examine the structural changes associated with loss of water molecules occurring for $[Zn(CH_3O–CO–C_6H_4COO)_2(OH_2)_3]\cdot 2H_2O$ in response to temperature rise.

During heating, dihydrated complex loses crystallization and coordination water molecules in successive steps, and then the anhydrous complex decomposes to ZnO. The solid products resulted from each thermal decomposition step were isolated and structurally characterized by means of elemental analysis and X-ray powder diffraction.

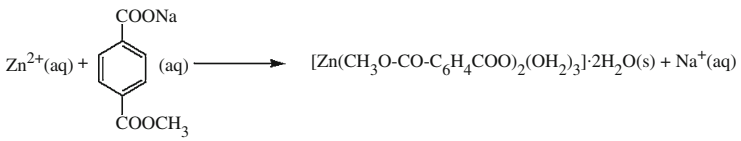

Experimental

Techniques and materials

Elemental analyses were carried out on a Heraeus CHNO-Rapid apparatus (Institute of Inorganic Chemistry, RWTH Aachen University).

Thermal analysis TG-DSC was followed with a Netzsch 449C STA Jupiter. Samples were placed in closed Al crucible and heated with 10 or 2 °C min^{-1}, under the flow of 20 mL min^{-1} dried air. An empty Al crucible was used as reference.

Powder X-ray diffraction (PXRD) patterns were recorded on a Stoe Stadi P diffractometer in transmission mode ($CuK\alpha_1$ radiation, Ge monochromator) with an image plate detector.

The temperature-dependent measurements were taken on a Guinier diffractometer (Huber G644, $CuK\alpha_1$ radiation, Ge monochromator) using samples sealed in 0.3-mm capillaries. The diffraction pattern acquisition was performed at fixed temperatures within the $30 < T < 400$ °C range every 5 °C for 10 min with a position-sensitive detector STOE PSD with a 2θ—range of 14° and an angular resolution of 0.02°.

SEM images were recorded on a SEM/EDAX high-resolution scanning electron microscope, Quanta Inspect F FEG (resolution 1.4 nm) with EDAX (133 eV resolution at MnKα)—FEI Company.

Synthesis of $[Zn(CH_3O–CO–C_6H_4COO)_2(OH_2)_3]\cdot 2H_2O$

Colorless crystals of $[Zn(CH_3O–CO–C_6H_4COO)_2(OH_2)_3]\cdot 2H_2O$ have been obtained by slow evaporation in air of aqueous mixture of $Zn(NO_3)_2\cdot 6H_2O$ (1 eq) and $C_9H_7O_4Na$ (1 eq), as described by us previously [10]:

For molecular formula $[Zn(C_9H_7O_4)_2(OH_2)_3]\cdot 2H_2O$, calcd (%): C 42.08, H 4.71; found: C 42.10, H 4.37.

Results and discussion

Thermal study (TG-DSC)

Thermal decomposition of aliphatic and aromatic carboxylates of Zn^{II} represents a convenient way, due to its

simplicity, low cost chemicals and reproducibility, to obtain ZnO with particle sizes in nanometer range.

A literature survey on decomposition processes of Zn^{II} aliphatic and aromatic carboxylates [20–27] showed that in all cases, in air atmosphere, ZnO was found as the final product. Regardless the nature of carboxylate ligand, thermal decomposition for hydrated compounds starts with the release of water molecules, and then anhydrous Zn^{II} complex decomposes on heating to ZnO. However, crystal structure and morphology of the zinc oxide particles [28, 29] depend on the decomposition temperature of complex and, implicitly, on the nature of organic ligand.

The proposed pathway for thermal decomposition of the title complex together with TG-DSC curves over the whole temperature range (25–530 °C) is given in Fig. 2 (Supplementary material Fig. S1).

The TG curve for the title complex exhibits three major decomposition steps (Fig. 2). The first step, with a mass loss of 14.08 %, takes place between 70 and 110 °C and can be attributed to the loss of four water molecules. The last water molecule is released in a slow endothermic process between 110 and 210 °C, the experimental mass loss being 3.85 %. In the interval 210–280 °C, a negligible mass loss is observed, but no additional process is detected.

The proposed formula for the complex isolated at $T = 280$ °C is $[Zn(CH_3O–COC_6H_4COO)_2]$.

$[Zn(C_9H_7O_4)_2]$, calcd (%): C 51.03, H 3.33; found: C 48.72, H 2.93.

The next succession of decomposition steps is attributed to the ligand degradation. Between 280 and 330 °C, a mass loss of 28.09 %, accompanied by a weak endothermic effect on DSC curve, corresponds roughly to the elimination of a $CH_3OOC–C_6H_4$ moiety. This step is followed by another slow decomposition process (8.80 %), between 330 and 405 °C, corresponding to the elimination of one CO_2 molecule. The remaining organic part is oxidized in the 440–510 °C temperature range. The mass loss (29.40 %) process is accompanied by a strong exothermic effect and is followed by the formation ($T > 510$ °C) of zinc oxide (ZnO) as the final product of the thermal decomposition. The total experimental mass loss of 84.80 % is in very good agreement with the theoretical mass loss, 84.23 %, deduced from the overall thermal decomposition process leading to ZnO.

In order to have a further insight of the first decomposition step, we carried out thermal decomposition experiment with a slower heating rate of 2 °C min^{-1} (inset of Fig. 2).

The DSC peaks indicate that the removal of the water molecules is a stepwise process. The first two endothermic peaks (at $T = 76$ °C and $T = 81.2$ °C, Fig. 2 inset) were attributed to the release of crystallization water molecules—dehydration process ($T = 76$ °C)—and to the loss of the labile water molecule from the apical position ($T = 81.2$ °C), respectively (exp. 10.45 %, calcd. 10.53 %, corresponding to the mass loss of three water molecules). As we already described [10], Zn1–O5 bond length is longer and presumably weaker than other Zn–O bonds in this complex, thus explaining the facile loss of the apical water molecule.

The proposed formula for the complex isolated at $T = 81.2$ °C is $[Zn(CH_3O–CO–C_6H_4COO)_2(OH_2)_2]$.

$[Zn(C_9H_7O_4)_2(OH_2)_2]$, calcd (%): C 47.03, H 3.95; found: C 47.65, H 4.30.

Successive endothermic processes, with the strongest effect at 83.6 °C, were observed in the DSC curve, and the associated mass loss (3.63 %) determined between 81.2 and 106.8 °C was consistent with the loss of one of the remaining equatorial water molecules.

The proposed formula for the complex isolated at $T = 106.8$ °C is $[Zn(CH_3O–CO–C_6H_4COO)_2(OH_2)]$.

$[Zn(C_9H_7O_4)_2(OH_2)]$, calcd (%): C 48.95, H 3.65; found: C 48.03, H 3.70.

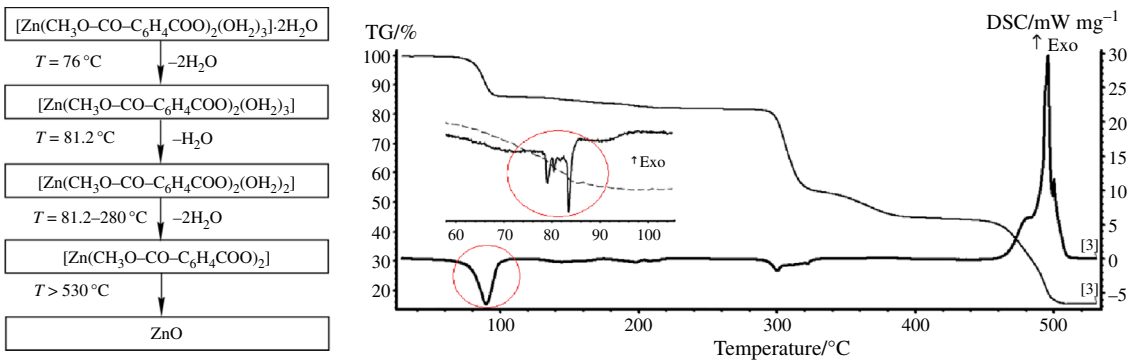

Fig. 2 TG-DSC curves for $[Zn(CH_3O–CO–C_6H_4COO)_2(OH_2)_3]·2H_2O$ over the whole temperature range (25–530 °C), at 10 °C min^{-1} heating speed. *Inset* graph: DSC curve for $[Zn(CH_3O–CO–C_6H_4COO)_2(OH_2)_3]·2H_2O$ over the temperature range 60–120 °C at 2 °C min^{-1} heating speed

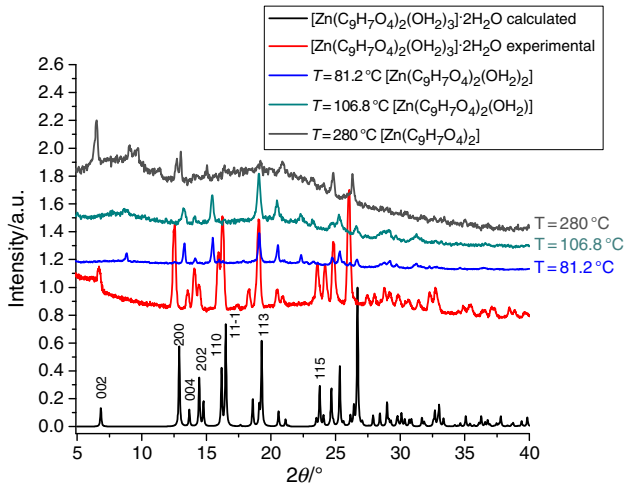

Fig. 3 XRD patterns, calculated and experimental, of $Zn(CH_3O–CO–C_6H_4COO)_2(OH_2)_3]\cdot 2H_2O$. The XRD patterns (normalized) of $Zn(CH_3O–CO–C_6H_4COO)_2(OH_2)_3]\cdot 2H_2O$ at dehydration/decomposition temperatures from TG-DSC; the experimental patterns were shifted by 0.6–1.2 *y*-units

XRD and T-XRD studies on the dehydration of $[Zn(C_9H_7O_4)_2(OH_2)_3]\cdot 2H_2O$

In Figs. 3 and 4, the XRD patterns of decomposition steps of $[Zn(C_9H_7O_4)_2(OH_2)_3]\cdot 2H_2O$ are shown.

For the decomposition compounds, isolated at $T = 81.2$ °C, $T = 106.8$ °C and $T = 280$ °C, XRD patterns show diffraction peaks reminiscent of ordered, crystalline structure of the starting complex $[Zn(C_9H_7O_4)_2(OH_2)_3]\cdot 2H_2O$ (Fig. 3).

In Fig. 4, the temperature-dependent XRD patterns of a powdered sample of $[Zn(CH_3O–CO–C_6H_4COO)_2(OH_2)_3]\cdot 2H_2O$ are shown. Beside the lattice parameter expansion with increasing temperature at 75 °C (endothermic effect on DSC curve), a structural change is detected that can be attributed to the loss of water in the crystal, also visible in the thermal study. At 120 °C, a sudden decrease in the lattice parameters is observed, explainable by the loss of water molecules without a structural change. A small change in reflection intensity can be attributed to further loss of water molecules. At 310 °C, a broadening of the reflections and a decreasing intensity were found in the XRD, which were correlated with the complete loss of water detected in the thermal analysis and also correspond to the start of the degradation process of the monomethyl terephthalate ligand.

As the thermal studies revealed, at temperatures higher than ~300 °C, the decomposition of the remaining complex fragment $\{[Zn(CH_3O–CO–C_6H_4COO)_2]\}$ occurred and the overall thermal decomposition process leads to ZnO. The formation of ZnO, detected in TG-DSC, has been confirmed by XRD, SEM and EDX analyses performed on the final product (Figs. 5 and 6).

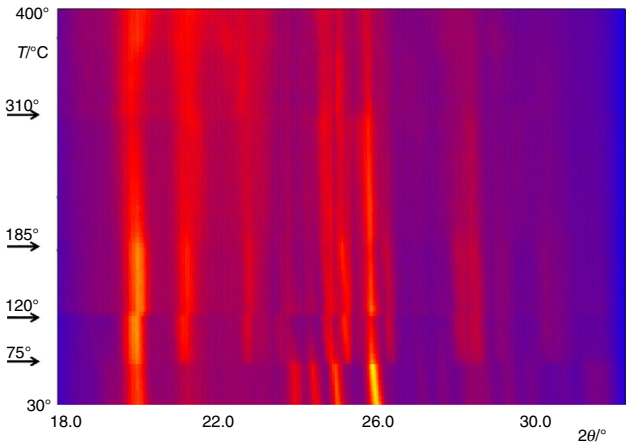

Fig. 4 Temperature-dependent XRD pattern of the dehydration of $[Zn(CH_3O–CO–C_6H_4COO)_2(OH_2)_3]\cdot 2H_2O$ from 30 to 400 °C

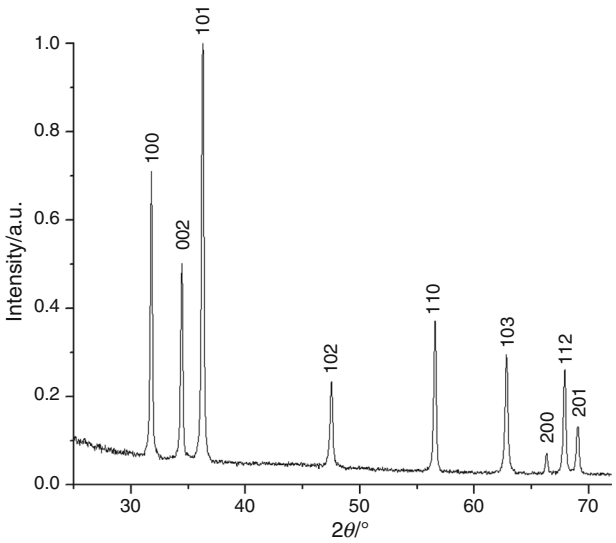

Fig. 5 XRD pattern of ZnO, hexagonal phase, space group $P6_3mc$

XRD pattern for the final product consists of ZnO pure phase, and no characteristic peaks are observed for other impurities.

The obtained ZnO is of wurtzite structure (hexagonal phase, space group $P6_3mc$); unit cell parameters $a = b = 3.25$ Å and $c = 5.18$ Å. In the XRD pattern of ZnO, all the diffraction peaks are well assigned to hexagonal phase ZnO reported in JCPDS card (number 36-1451). Crystallite size of 33 nm was calculated by using Scherrer formula for the most intense peak corresponding to 101 plane located at 36.255°.

SEM and EDX

The SEM images reveal that the product consists of spherical particles with the average size of 58 nm which, taking into account the crystallite size estimated by

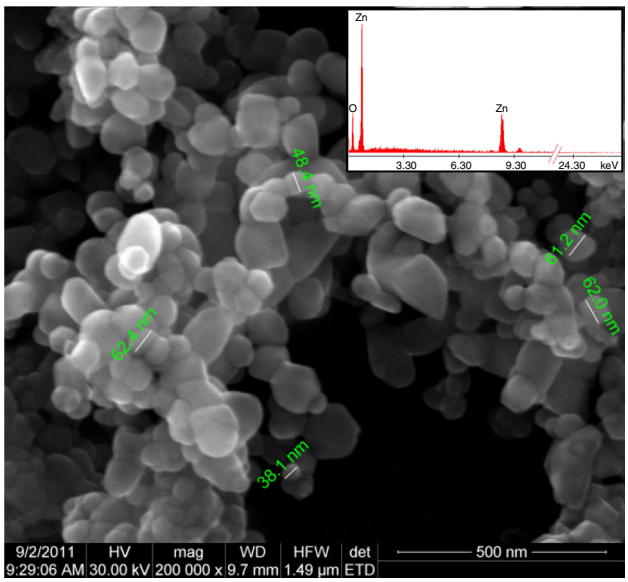

Fig. 6 SEM/EDX (*inset* picture) images of ZnO

Scherrer formula from the XRD pattern, suggests that the particles are either single crystallites or composed of two individual crystallites. Moreover, the EDX pattern confirms that the isolated ZnO is pure and contains only zinc and oxygen.

Conclusions

Thermal decomposition and thermo-X-ray diffraction analyses of a Zn^{II} monomethyl terephthalate complex, $[Zn(CH_3O–CO–C_6H_4COO)_2(OH_2)_3]\cdot 2H_2O$, are reported in this paper. The structural changes associated with loss of water molecules for $[Zn(CH_3O–CO–C_6H_4COO)_2(OH_2)_3]\cdot 2H_2O$ in response to the increase in temperature were examined.

XRD patterns for isolated compounds of decomposition steps lead us to conclude that the reminiscent ordered structure of crystalline complex is preserved below 300 °C. This behavior suggests that the labile water ligands from our title complex might be further replaced by other ligands with different hydrogen bonding characteristics and therefore the dimensionality of the structure could be modulated.

Dihydrated complex loses crystallization and coordination water molecules in successive steps, and then the anhydrous complex decomposes to ZnO, spherical nanoparticles with the average size of 58 nm being obtained as the SEM analysis pointed out. Due to the wide application of ZnO in various fields, this simple and reproducible synthesis route toward ZnO nanoparticles with high purity and excellent yield could be efficient.

Acknowledgements Authors recognize financial support from the European Social Fund through POSDRU/89/1.5/S/54785 project: Postdoctoral Program for Advanced Research in the field of nanomaterials.

References

1. Rao CNR, Natarajan S, Vaidhyanathan R. Angew Chem Int Ed. 2004;43:1466–96.
2. Cui Y, Evans OR, Ngo HL, White PS, Lin W. Angew Chem Int Ed. 2002;41:1159–62.
3. Baca SG. IJPAC-Int Res J Pure Appl Chem. 2012;2(1):1–24.
4. Kitagawa S, Kitaura R, Noro S-i. Angew Chem Int Ed. 2004;43:2334–75.
5. Mori W, Sato T, Ohmura T, Kato CN, Takei TJ. Solid State Chem. 2005;178:2555–73.
6. Mori W, Takamizawa S. J. Solid State Chem. 2000;152(10):120–9.
7. Li H, Eddaoudi M, O'Keeffe M, Yaghi OM. Nature. 1999;402:276–9.
8. Hawxwell SM, Adams H, Brammer L. Acta Cryst. 2006;B62:808–14.
9. Acheson RJ, Galwey AK. J. Chem. Soc. A 1967;1174–1178.
10. Şerb M-D, Wang Y, Dumitru F, Englert U. Acta Cryst. 2011;E67:m475–6.
11. Li H, Eddaoudi M, Groy TL, Yaghi OM. J Am Chem Soc. 1998;120:8571–2.
12. Clausen HF, Poulsen RD, Bond AD, Chevallier M-AS, Iversen BB. J Solid State Chem. 2005;178:3342–51.
13. Sun J, Zhou Y, Fang Q, Chen Z, Weng L, Zhu G, Qiu S, Zhao D. Inorg Chem. 2006;45:8677–84.
14. Yin P-X, Zhang J, Li Z-J, Qin Y-Y, Cheng J-K, Yao Y-G. Inorg Chem Commun. 2008;11:134–7.
15. Carton A, Mesbah A, Aranda L, Rabu P, Francois M. Solid State Sci. 2009;11:818–23.
16. Roy S, Sarkar BN, Bhar K, Satapathi S, Mitra P, Ghosh BK. J Mol Str. 2013;1037:160–9.
17. Donald Kirkbright Black, US Patent 4058663, 1977.
18. Tranchemontagne DJ, Mendoza-Cortés JL, O'Keeffe M, Yaghi OM. Chem Soc Rev. 2009;38:1257–83.
19. Spek AL. Acta Cryst. 2009;D65:148–55.
20. Brzyska W, Wańczowska-Fonfara D. J Therm Anal Calorim. 1989;35(3):727–33.
21. Carp O, Patron L, Segal E. Rev Roum Chim. 2006;51(1):5–12.
22. Findoráková L, Györyová K, Hudecová D, Mudroňová D, Kovářová J, Homzová K, Nour El-Dien FA. J Therm Anal Calorim. 2013;111:1771–81.
23. Bujdošová Z, Györyová K, Kovářová J, Hudecová D, Halás L. J Therm Anal Calorim. 2009;98:151–9.
24. Brzyska W, Ozga W. J Therm Anal Calorim. 2002;67:623–9.
25. Skoršepa J, Godočíková E, Černák J. J Therm Anal Calorim. 2004;75:773–80.
26. Kurpiel-Gorgol R, Brzyska W. J Therm Anal Calorim. 2003;71:539–48.
27. Krajníková A, Györyová K, Kovářová J, Hudecová D, Hubáčková J, Nour El-Dien F, Koman M. J Therm Anal Calorim. 2012;110(1):177–85.
28. Morkoç H, Özgur Ü, Zinc oxide: fundamentals, materials and device technology. Wiley. KGaA, Weinheim: GmbH & Co; 2009. ISBN 978-3-527-40813-9.
29. Wang ZL. J Phys Condens Matter. 2004;16:R829.